DOI: 10.1002/chem.200600424

Formation and Stability of G-Quadruplexes Self-Assembled from Guanine-Rich Strands

Jiang Zhou,[a] Gu Yuan,*[a] Junjun Liu,[b] and Chang-Guo Zhan[b]

Abstract: Electrospray ionization mass spectrometry (ESI-MS) was utilized to investigate the formation and stability of G-quadruplexes. For the 15 6-nt oligonucleotides tested, ESI-MS indicated that formation of a parallel tetramer quadruplex requires at least four continuous guanines in the 6-nt sequence. In addition, the G-rich strands prefer to employ "self-association" in the formation of the G-quadruplex rather than hybridized integration, and the thermodynamic-stability order of these three G-quadruplexes is Q(2) > Q(1) > Q(3).

Keywords: DNA · G-quadruplexes · polyamides · self-assembly · telomeric DNA

Introduction

Guanine-rich sequences exist in many important DNA regions, such as promoter regions of some oncogenes, centromeres, and especially telomeres. Telomeres are repeats of G-rich sequences consisting of $(TGGGGT)_n$ in *Tetrahymen*, $(TTAGGG)_n$ in human, and $(TTTTGGGG)_n$ in *Oxytricha*.[1,2] The oligonucleotides with G-rich sequences can form four-stranded G-quadruplexes (Figure 1A).[3,4] Telomeric DNA sequences have several functions essential for genome integrity, and the formation of these quadruplexes has been shown to decrease the activity of the enzyme telomerase, which is responsible for elongating telomeres.[5] Therefore, the G-quadruplex structures have become a potential target for the development of genetic-based anticancer drugs.[6,7] Understanding the factors affecting the formation and stability of G-quadruplexes could also contribute considerably to the construction of potential nanomolecular devices.[8–10]

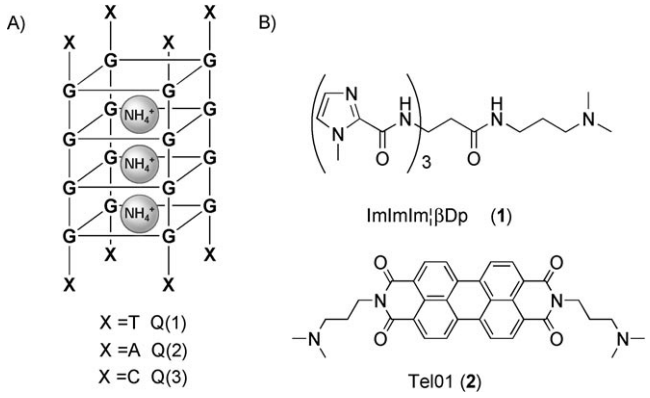

Figure 1. A) Three important G-quadruplex structures. B) Structures of two DNA binders. Im: *N*-methylimidazole; β: β-alanine; Dp: 3-(dimethylamino)propylamine.

Although NMR, X-ray, and CD spectroscopies have provided the structure information of G-quadruplexes, they cannot be applied in some complicated cases, such as mixtures of several different quadruplexes. Accordingly, in this study, we utilized electrospray ionization mass spectrometry (ESI-MS)[11–15] to investigate the formation and stability of G-quadruplexes, as this offers direct views of distinct quadruplex peaks rapidly and simultaneously. Meanwhile, in consideration of the stabilization of a G-quadruplex by binding molecules, we investigated the binding affinity of two DNA-recognition molecules, polyamide (**1**) and Tel01 (**2**), with the G-quadruplexes (Figure 1B). Polyamide is a novel DNA-recognition molecule and has good cell permeation, whereas

[a] Dr. J. Zhou, Prof. Dr. G. Yuan
Beijing National Laboratory for Molecular Sciences
Key Laboratory of Bioorganic Chemistry and
Molecular Engineering of Ministry of Education
Department of Chemical Biology
College of Chemistry and Molecular Engineering
Peking University, Beijing 100871 (China)
Fax: (+86) 10-6275-1708
E-mail: guyuan@pku.edu.cn

[b] J. Liu, Prof. Dr. C.-G. Zhan
Department of Pharmaceutical Sciences
College of Pharmacy, University of Kentucky
725 Rose Street, Lexington, KY 40536 (USA)

Supporting information for this article is available on the WWW under http://www.chemeurj.org/ or from the author.

Tel01 contains a huge aromatic system in favor of π stacking with G-quartets.[16–19]

Results and Discussion

Formation of the G-quadruplexes: Firstly, we chose 15 6-nt oligonucleotides with different sequences and studied the formation of the G-quadruplexes (Table 1). The ESI-MS spectra revealed only three G-quadruplex peaks associated with these sequences; d(TGGGGT) [Q(1)], d(AGGGGA) [Q(2)], and d(CGGGGC) [Q(3)] (Figure 2), indicating that formation of a parallel tetramer quadruplex requires at least four continuous guanines in the 6-nt sequence. These experimental observations are consistent with the relative binding free energies ($\Delta\Delta G$, also listed in Table 1) estimated by computational modeling at $T=298.15$ K and $P=1$ atm (see Computational Modeling section for details).

The $\Delta\Delta G$ value for a given G-quadruplex Q(X) formed from the corresponding single strand S(X) was evaluated relative to the binding free energy of Q[d(CGGGGC)], that is, $\Delta\Delta G\{Q(X)\}=\Delta G\{Q(X)\}-\Delta G\{Q[d(CGGGGC)]\}=[G\{Q(X)\}-4\times G\{S(X)\}]-[G\{Q[d(CGGGGC)]\}-4\times G\{S[d(CGGGGC)]\}]$. In this equation, $\Delta G\{Q(X)\}$ and $\Delta G\{Q[d(CGGGGC)]\}$ are the Gibbs binding free energies of quadruplexes Q(X) and Q[d(CGGGGC)], respectively. $G\{Q(X)\}$ and $G\{Q[d(CGGGGC)]\}$ represent the Gibbs free energies of quadruplexes Q(X) and Q[d(CGGGGC)], respectively, and $G\{S(X)\}$ and $G\{S[d(CGGGGC)]\}$ refer to the Gibbs free energies of single strands S(X) and S[d(CGGGGC)], respectively. The Gibbs free energies of all the structures were calculated by using the molecular mechanics Poisson–Boltzmann surface-area (MM-PBSA) free-energy approach implemented in the popular AMBER 8 program suite.[20] All of the quadruplex structures were energy-minimized prior to performing the MM-PBSA free-energy calculations. The calculated relative binding free energies (Table 1) reveal that the quadruplexes corresponding to Q(1) and Q(2) are more stable than the quadruplex corresponding to Q(3), and that all of the other 12 hypothetical quadruplexes are less stable than the quadruplex corresponding to Q(3). These results suggest the stability order of the 15 hypothesized quadruplexes to be Q(2) > Q(1) > Q(3) > all others, which explains why only three quadruplexes corresponding to Q(1), Q(2), and Q(3) were observed, and why Q(2) is the most stable quadruplex ob-

Table 1. Quadruplex formation and the calculated relative binding free energies ($\Delta\Delta G$ [kcal mol^{-1}] at $T=298.15$ K and $P=1$ atm) of the hypothesized G-quadruplexes.

Sequence	G(Complex)	G(Monomer)	$G(NH_4^+)$	$\Delta\Delta G$ (calcd)[a]	Structure observed[b]
5′-AGGGGA-3′	−5936.2	−1417.0	−107.1	−57.9	Q(2)
5′-TGGGGT-3′	−5587.3	−1339.2	−107.1	−20.1	Q(1)
5′-CGGGGC-3′	−6549.0	−1584.7	−107.1	0	Q(3)
5′-TTGGTT-3′	−4783.0	−1149.0	−107.2	23.8	S, D
5′-TTGGGT-3′	−5144.5	−1241.6	−107.2	32.8	S, D
5′-TCGGGT-3′	−5625.7	−1363.4	−107.1	38.3	S, D
5′-ACCCCA-3′	−6245.2	−1520.2	−107.1	45.9	S, D
5′-TGCCGT-3′	−5682.9	−1385.4	−107.0	68.5	S, D
5′-TCGGCT-3′	−5708.6	−1393.8	−107.1	76.8	S, D
5′-CCGGCC-3′	−6661.5	−1634.5	−107.2	87.0	S, D
5′-TCGCCT-3′	−5796.2	−1420.6	−107.0	96.2	S, D
5′-TGTGTT-3′	−4717.7	−1154.7	−107.0	111.3	S, D
5′-TGTGGT-3′	−5087.3	−1248.1	−107.0	115.3	S, D
5′-TGCGGT-3′	−5538.3	−1365.6	−107.1	134.4	S, D
5′-TCGCGT-3′	−5639.7	−1394.7	−107.2	149.8	S, D

[a] The $\Delta\Delta G$ value was relative to the binding free energy of the G-quadruplex formed from d(CGGGGC) [Q(3)]. [b] Q(X) = quadruplex; S = single strand; D = duplex; from ESI-MS spectra.

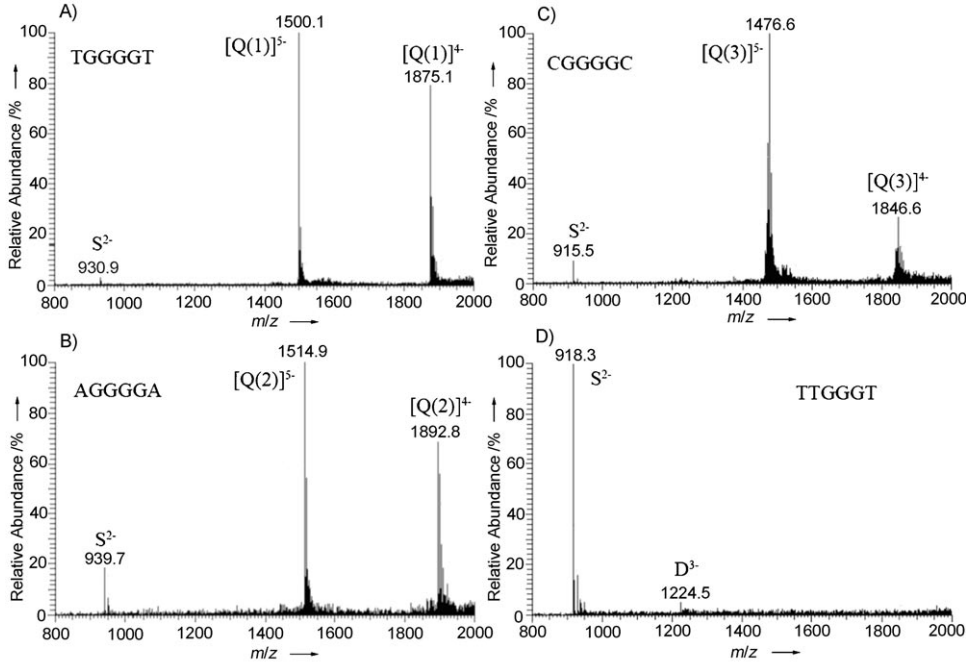

Figure 2. ESI mass spectra of four potential 6-nt quadruplex sequences. S, single strand; D, duplex; Q, quadruplex. A) TGGGGT; B) AGGGGA; C) CGGGGC; D) TTGGGT.

served. This may also be because A moieties have the ability to stack above and below the G-quartets, thereby stabilizing the quadruplex, whereas C and T bases stack less readily than A.

Furthermore, based on the quadruplex peaks (5− charge state of TG_nT, $n=4$–8) in mass spectra, we found that the number of ammonium ions increased in parallel with the number of guanines, according to the "$n-1$" rule ($n=$ number of guanines), indicating that each ammonium ion is located between the G-tetrads.

Mixtures of oligonucleotides with different sequences: Upon mixing d(TGGGGT), d(AGGGGA), and d(CGGGGC), no heteroquadruplex was observed; three peaks ($m/z=1476.8$, 1500.0, and 1514.3 corresponding to Q(1), Q(2), and Q(3), respectively) are presented in the ESI mass spectrum (Figure 3A). In addition, the ESI mass spectra recorded for the mixtures of d(TGGGGT), d(AGGGGA), and d(CGGGGC) with other similar 6-nt oligonucleotides also did not reveal any peak associated with a heteroquadruplex (Figure 3B). This interesting "self-association" phenomenon is the first observed by using mass spectrometry, which is the only way to investigate the respective structures in a mixture of several oligonucleotides.

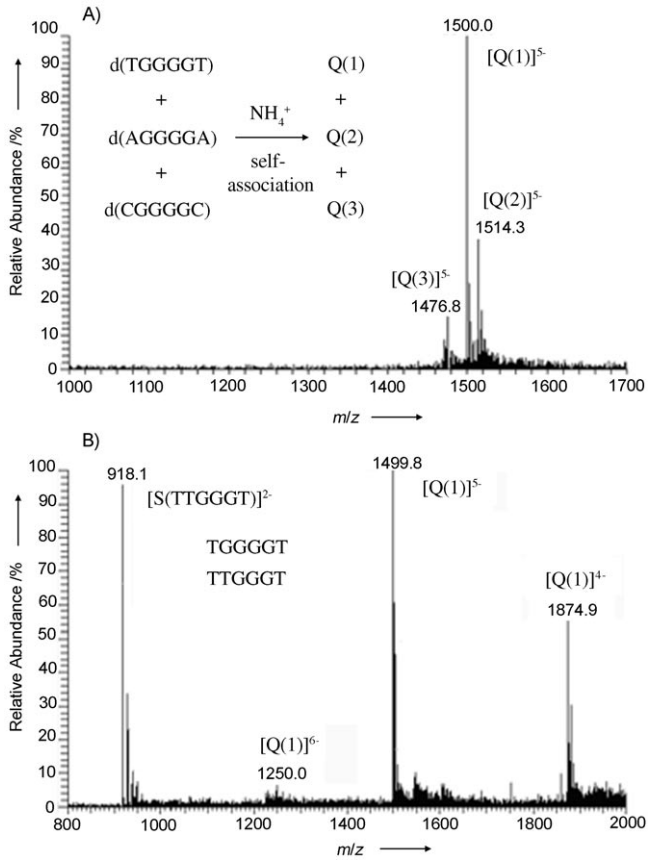

Figure 3. ESI mass spectra showing "self-association" formation of G-quadruplexes. S, single strand; D, duplex; Q, quadruplex. A) Mixture of TGGGGT, AGGGGA, and CGGGGC; B) mixture of TGGGGT and TTGGGT.

To better understand this experimental observation, we also used the aforementioned MM-PBSA free-energy approach to estimate the free energies (ΔG) of various reactions (Table 2), such as the following (as examples):

$$3\{[S(1)]_4\} + \{[S(2)]_4\} \rightarrow 4\{[S(1)]_3[S(2)]_1\} \quad (1)$$

$$\{[S(1)]_4\} + 3\{[S(2)]_4\} \rightarrow 4\{[S(1)]_1[S(2)]_3\} \quad (2)$$

$$3\{[S(1)]_4\} + \{[S(3)]_4\} \rightarrow 4\{[S(1)]_3[S(3)]_1\} \quad (3)$$

$$\{[S(1)]_4\} + 3\{[S(3)]_4\} \rightarrow 4\{[S(1)]_1[S(3)]_3\} \quad (4)$$

$$3\{[S(2)]_4\} + \{[S(3)]_4\} \rightarrow 4\{[S(2)]_3[S(3)]_1\} \quad (5)$$

$$\{[S(2)]_4\} + 3\{[S(3)]_4\} \rightarrow 4\{[S(2)]_1[S(3)]_3\} \quad (6)$$

Table 2. The calculated absolute free-energy changes [kcal mol^{-1}] of the hypothesized heteroquadruplexes.

Structure[a]	E(Total)	TS	G	ΔG
5′-AGGGGA-3′ complex	−5296.72	639.49	−5936.21	–
5′-CGGGGC-3′ complex	−5922.64	626.38	−6549.02	–
5′-TGGGGT-3′ complex	−4950.09	637.25	−5587.34	–
3A1C complex	−5429.05	632.07	−6061.12	113.17
3A1T complex	−5200.84	636.83	−5837.67	45.29
3C1 A complex	−5761.04	624.98	−6386.02	39.19
3C1T complex	−5679.44	628.29	−6307.74	3.44
3T1 A complex	−5030.84	636.86	−5667.70	27.43
3T1C complex	−5188.70	634.10	−5822.81	19.80

[a] A represents strand 5′-AGGGGA-3′, T refers to 5′-TGGGGT-3′, and C represents 5′-CGGGGC-3′. The 5′-AGGGGA-3′ complex consists of four 5′-AGGGGA-3′ strands. The 3A1C complex consists of three 5′-AGGGGA-3′ strands and one 5′-CGGGGC-3′ strand. Other complexes are defined in the same way. The positive free-energy changes suggest that only homoquadruplexes can exist, as the heteroquadruplexes tend to form homoquadruplexes.

In reactions (1) to (6), S(1), S(2), and S(3) represent the single strands (i.e., TGGGGT, AGGGGA, and CGGGGC) that form the heteroquadruplexes Q(1,2), Q(1,3), and Q(2,3), respectively. The calculated free energies of all these reactions are positive values, for example, $\Delta G(1)=27.4$, $\Delta G(2)=45.3$, $\Delta G(3)=19.8$, $\Delta G(4)=3.4$, $\Delta G(5)=113.2$, and $\Delta G(6)=39.2$ kcal mol^{-1}. Both the calculated and the experimental data demonstrate consistently that the G-rich strands prefer to employ "self-association" in the formation of the G-quadruplexes rather than hybridized integration. Similarly, our current study with 8–12-nt oligonucleotides also provided proof of these phenomena.

Binding affinities of binders with the quadruplexes: To examine the effects of binding molecules on the stabilization of the G-quadruplex, the binding stoichiometries and affinities were studied by mixing quadruplex Q(1) with binders **1** and **2** in different molar ratios ranging from Q(1):binder = 1:1 to 1:8 (Figure 4A,B). For **1**, the ESI-MS spectra show ion peaks for [Q(1)+1 binder], [Q(1)+2 binders], [Q(1)+3 binders], and [Q(1)+4 binders]; and in the case of **2**, [Q(1)+3 binders] and [Q(1)+4 binders] ions were not ob-

served, even at higher molar ratios. Here, the abundance ratio (R_m, $m=1$–4; $m=$number of binders in the complex) of the complex to Q(X), $[complex]^{5-}/[Q(X)]^{5-}$, was defined as a unique parameter for the evaluation of the binding affinities of **1** and **2**, and was calculated directly from the abundances in ESI mass spectra. The R_m was determined at four different molar ratios and the results are shown in Table 3. The R_m value of **2** is much greater than that of **1**. This indicates that **2** is an excellent binder for the quadruplex. For Q(2) and Q(3), similar binding orders were obtained. By comparing the binding of three quadruplexes with **2** (Figure 4B–D), we found that Q(2) > Q(1) > Q(3). In addition, our further study indicated that **2** had a specific selectivity to quadruplexes in the presence of duplex telomeric DNA.

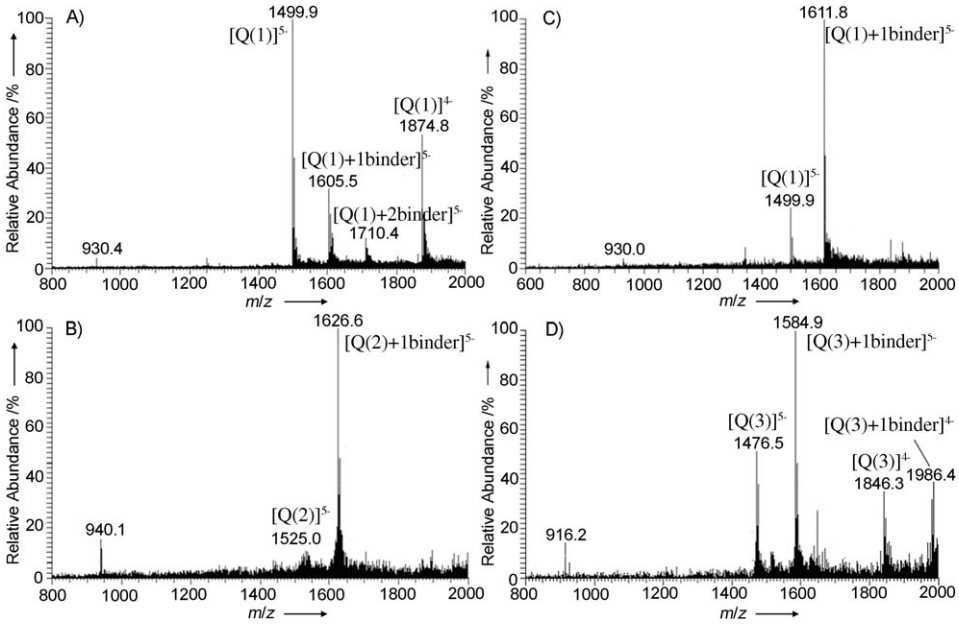

Figure 4. ESI mass spectra of quadruplexes with the binders, molar ratio = 1:1. A) Q(1) with ImImImβDp (**1**); B) Q(1) with Tel01 (**2**); C) Q(2) with Tel01 (**2**); D) Q(3) with Tel01 (**2**).

Table 3. The abundance ratios R_m of complexes with Q(1) at four different molar ratios.[a]

Molar ratio	**1**				**2**	
	R_1	R_2	R_3	R_4	R_1	R_2
1:1	0.47	0.13	0.00	0.00	3.33	0.00
1:2	0.88	0.43	0.12	0.00	9.09	2.27
1:4	1.22	0.62	0.24	0.11	nq	nq
1:8	3.13	1.94	0.88	0.56	nq	nq
average	1.42	0.78	0.31	0.17	6.21	1.14

[a] nq = not quantified.

Stabilization of complexes of G-quadruplex and binders: The stabilization of complexes of G-quadruplex and binders **1** or **2** was investigated by performing assays at increasing temperature. As the capillary temperature of mass spectrometry was increased from 70 to 400 °C (400 °C is the upper limit of the capillary temperature, and below 70 °C the effect of desolvation is significant), single-stranded ions were observed, and the signals of the quadruplex and complex ions became weaker and finally disappeared. Here, P is defined as the proportion of single-stranded DNA for the evaluation of the thermodynamic stability of the complexes

$$P = \sum [S(X)]^{n-} / \{\sum [Q(X)]^{n-} + \sum [complex]^{n-}\}$$

in which $n=4$ and 5. If $P=1$, the corresponding temperature ($T_{P=1}$) was taken as a parameter to evaluate the stability. The $T_{P=1}$ values are shown in Table 4. The data in Table 4 show that the binding molecules can stabilize the quadruplex–complex structures. The stronger the quadruplex–binder interaction, the more stable the complex. Moreover, the thermal-stability order of the three quadruplexes can be evaluated as Q(2) > Q(1) > Q(3), and the stabilization of $[Q(2)+\mathbf{2}]^{5-}$ is the highest of these complexes.

Table 4. The $T_{P=1}$ values determined for the quadruplexes and the quadruplex–binder complexes.

	$T_{P=1}$		$T_{P=1}$		$T_{P=1}$
Q(1)	300	Q(2)	310	Q(3)	240
Q(1)+**1**	310	Q(2)+**1**	320	Q(3)+**1**	280
Q(1)+**2**	330	Q(2)+**2**	340	Q(3)+**2**	310

Conclusion

We utilized electrospray ionization mass spectrometry (ESI-MS) to investigate the formation and stability of G-quadruplexes. The ESI-MS spectra revealed only three G-quadruplex peaks associated with these sequences, and the stability order was evaluated to be Q(2) > Q(1) > Q(3). Both the calculated and the experimental data demonstrate consistently that the G-rich strands prefer to employ "self-association" in the formation of the G-quadruplexes rather than hybridized integration. Furthermore, we compared the binding affinity of two binders (**1** and **2**) with the G-quadruplexes, and determined that the orders of both the binding and stability of the G-quadruplexes are **2** > **1**. This method can also be applied to other telomeric DNA structures. Our current studies focusing on human telomeric DNA have provided some significant results that will provide a valuable basis for the future rational design of genetic-based anticancer drugs.

Experimental Section

Oligodeoxyribonucleotides: Single-stranded oligonucleotides were purchased from Augct (Beijing, China) and were dissolved directly in deionized water. The resulting DNA stock solution was 500 μM in deionized water, which ensured that the mixing assays started with single strands.

Ligand synthesis: A haloform reaction was used to synthesize polyamide (**1**) (yield 65%), and the purification and characterization of **1** was performed according to our previous paper.[19] Perylene derivative Tel01 (**2**) was synthesized by refluxing a mixture of 3,4,9,10-perylenetetracarboxylic dianhydride and 3-(dimethylamino)propylamine (Dp) (yield 86%).

Mixing and binding assays: Oligonucleotides were stored as stock solutions in deionized water. After thawing, each DNA stock solution (2.0 μL) was mixed, then diluted with methanol/100 mM ammonium acetate (20:80, v/v) to a volume of 40 μL (final conc. of each DNA = 25 μM). Binding molecules were dissolved in a mixture of methanol/water (50:50, v/v) to a concentration of 500 μM. Each DNA solution (2.0 μL) was mixed with 2.0–16 μL of binder solutions, and then diluted with methanol/100 mM ammonium acetate (20:80, v/v) to a final volume of 40 μL. Methanol was added to obtain a good spray.[12]

Mass spectrometry: ESI-MS spectra were obtained in the negative-ion mode by using a Thermo Finnigan LCQ Deca XP Plus ion-trap mass spectrometer (San Jose, CA). The oligonucleotide solutions were infused directly into the ion source at a flow rate of 2 μL min^{-1}. The electrospray source conditions were: 2.0–2.5 kV spray voltage, 100 °C capillary temperature, and a double-sheath gas (20 arb) to ensure efficient desolvation. Data were collected and analyzed by using the Xcalibur software developed by Thermo Finnigan, and ten scans were averaged for each spectrum.

Computational modeling: The X-ray structure of parallel-stranded guanine tetraplex (PDB entry 244D) was selected as the template to construct the initial structures used for the molecular mechanics Poisson–Boltzmann surface-area (MM-PBSA)[21,22] calculations. Prior to the MM-PBSA energy calculations, the structures of 15 hypothesized G-quadruplexes and six heteroquadruplexes were constructed by using the LEaP module of the AMBER 8 program suite.[20] The restrained electrostatic-potential (RESP) charges used for the NH_4^+ ion were calculated at the HF/6–31G* level by using the Gaussian 03 program.[23] Each of the structures was fully energy-minimized. After the energy minimizations, the solute energies were evaluated without using any cutoff for all of the structures. The same structures were used in the PBSA solvation-energy calculations by using the PBSA module of the AMBER 8 program suite. In the PBSA calculations, the grid size used was defined as 0.5 Å and the radius of the probe atom was set to 1.4 Å. The charges used in the Poisson–Boltzmann (PB) calculations were read from the AMBER topology parameters. The solvent-accessible surface (SAS) was obtained by using the molsurf module of the AMBER 8 program suite. In addition, the entropy contributions from the translations, rotations, and vibrations to the binding free energy were calculated by performing the standard normal-mode analyses on the energy-minimized structures by using the n-mode module of the AMBER 8 program suite. The Gibbs free energy G for each structure was calculated by using $G = E_{MM} + G_{PB} + G_{SA} - TS$ (see the AMBER 8 user manual for details).[20] The calculated free energies and the binding free energies are listed in Tables 1 and 2.

Acknowledgements

This work was supported in part by the National Natural Science Foundation of China (No. 20272005 and 20472009).

[1] V. A. Zakian, *Science* **1995**, *270*, 1601–1607.
[2] K. Collins, *Curr. Opin. Cell Biol.* **2000**, *12*, 378–383.
[3] G. N. Parkinson, M. P. H. Lee, S. Neidle, *Nature* **2002**, *417*, 876–880.
[4] F. Lavelle, J. F. Riou, A. Laoui, P. Mailliet, *Crit. Rev. Oncol. Hematol.* **2000**, *34*, 111–126.
[5] T. M. Fletcher, D. K. Sun, M. Salazar, L. H. Hurley, *Biochemistry* **1998**, *37*, 5536–5541.
[6] D. Hanahan, R. A. Weinberg, *Cell* **2000**, *100*, 57–70.
[7] E. M. Rezler, D. J. Bearss, L. H. Hurley, *Annu. Rev. Pharmacol. Toxicol.* **2003**, *43*, 359–379.
[8] M. Crnugelj, P. Sket, J. Plavec, *J. Am. Chem. Soc.* **2003**, *125*, 7866–7871.
[9] G. R. Clark, P. D. Pytel, C. J. Squire, S. Neidle, *J. Am. Chem. Soc.* **2003**, *125*, 4066–4067.
[10] A. Wong, R. Ida, L. Spindler, G. Wu, *J. Am. Chem. Soc.* **2005**, *127*, 6990–6998.
[11] K. X. Wan, T. Shibue, M. L. Gross, *J. Am. Chem. Soc.* **2000**, *122*, 300–307.
[12] V. Gabelica, E. De Pauw, F. Rosu, *J. Mass. Spectrom.* **1999**, *34*, 1328–1337.
[13] J. Zhou, G. Yuan, *Chem. Eur. J.* **2005**, *11*, 1157–1162.
[14] W. M. David, J. Brodbelt, S. M. Kerwin, P. W. Thomas, *Anal. Chem.* **2002**, *74*, 2029–2033.
[15] F. Rosu, V. Gabelica, C. Houssier, P. Colson, E. De Pauw, *Rapid Commun. Mass Spectrom.* **2002**, *16*, 1729–1736.
[16] P. B. Dervan, R. W. Burli, *Curr. Opin. Chem. Biol.* **1999**, *3*, 688–693.
[17] M. J. Cocco, L. A. Hanakahi, M. D. Huber, N. Maizels, *Nucleic Acids Res.* **2003**, *31*, 2944–2951.
[18] J. T. Kern, P. W. Thomas, S. M. Kerwin, *Biochemistry* **2002**, *41*, 11379–11389.
[19] J. H. Xiao, G. Yuan, W. Q. Huang, A. S. C. Chan, K. L. D. Lee, *J. Org. Chem.* **2000**, *65*, 5506–5513.
[20] AMBER 8 program suite, D. A. Case, T. A. Darden, T. E. Cheatham III, C. L. Simmerling, J. Wang, R. E. Duke, R. Luo, K. M. Merz, B. Wang, D. A. Pearlman, M. Crowley, S. Brozell, V. Tsui, H. Gohlke, J. Mongan, V. Hornak, G. Cui, P. Beroza, C. Schafmeister, J. W. Caldwell, W. S. Ross, P. A. Kollman, University of California, San Francisco, **2004**.
[21] E. Fadrna, N. Spackova, R. Stefl, J. Koca, T. E. Cheatham, J. Sponer, *Biophys. J.* **2004**, *87*, 227–242.
[22] D. L. Harris, J. Y. Park, L. Gruenke, L. Waskell, *Proteins* **2004**, *55*, 895–914.
[23] *Gaussian 03*, Revision A.1, M. J. Frisch, G. W. Trucks, H. B. Schlegel, G. E. Scuseria, M. A. Robb, J. R. Cheeseman, J. A. Montgomery, Jr., T. Vreven, K. N. Kudin, J. C. Burant, J. M. Millam, S. S. Iyengar, J. Tomasi, V. Barone, B. Mennucci, M. Cossi, G. Scalmani, N. Rega, G. A. Petersson, H. Nakatsuji, M. Hada, M. Ehara, K. Toyota, R. Fukuda, J. Hasegawa, M. Ishida, T. Nakajima, Y. Honda, O. Kitao, H. Nakai, M. Klene, X. Li, J. E. Knox, H. P. Hratchian, J. B. Cross, C. Adamo, J. Jaramillo, R. Gomperts, R. E. Stratmann, O. Yazyev, A. J. Austin, R. Cammi, C. Pomelli, J. W. Ochterski, P. Y. Ayala, K. Morokuma, G. A. Voth, P. Salvador, J. J. Dannenberg, V. G. Zakrzewski, S. Dapprich, A. D. Daniels, M. C. Strain, O. Farkas, D. K. Malick, A. D. Rabuck, K. Raghavachari, J. B. Foresman, J. V. Ortiz, Q. Cui, A. G. Baboul, S. Clifford, J. Cioslowski, B. B. Stefanov, G. Liu, A. Liashenko, P. Piskorz, I. Komaromi, R. L. Martin, D. J. Fox, T. Keith, M. A. Al-Laham, C. Y. Peng, A. Nanayakkara, M. Challacombe, P. M. W. Gill, B. Johnson, W. Chen, M. W. Wong, C. Gonzalez, J. A. Pople, Gaussian, Inc., Pittsburgh PA, **2003**.

Received: March 28, 2006
Revised: June 24, 2006
Published online: October 11, 2006

